Analyses of Extreme Wave Heights in the Gulf of Mexico for Offshore Engineering Applications

Vijay Panchang
Texas A&M University,
Maritime Systems Engineering Department,
200 Seawolf Parkway,
Galveston, TX 77553
e-mail: panchanv@tamug.edu

Chan Kwon Jeong
Dockwise USA,
16340 Park Ten Place,
Suite 200,
Houston, TX 77084
e-mail: chankwon.jeong@gmail.com

Zeki Demirbilek[1]
U.S. Army Engineer Research
and Development Center,
Coastal & Hydraulics Laboratory,
3909 Halls Ferry Road,
Vicksburg, MS 39180
e-mail: zeki.demirbilek@usace.army.mil

The 2004–2008 hurricane season in the Gulf of Mexico (GOM) saw several exceedances of what was regarded, prior to that period, as the 100-year significant wave heights (SWHs) that are used for the design of offshore oil and gas facilities. As a result, these facilities sustained considerable damage and disrupted U.S. energy supplies. The wave climatology in the GOM is therefore studied in detail. A 51-year database of SWHs was constructed by using a combination of wind and wave models, and both individual wave heights and statistical measures were validated, to the extent possible, using buoy data. Analyses of the modeled data show that there is an increasing trend in the annual maximum SWHs in the eastern part of the GOM; the maximum trend is approximately 5.6 cm/year, which is of the same magnitude as that reported for the U.S. west coast. The western part; on the other hand, shows a decreasing trend. The maximum estimated 100-year SWHs (denoted by SWH_{100}) are 19.1 m, 22.6 m and 26.7 m for the Gumbel, Weibull, and the GEV distributions, respectively. The estimates obtained here using the Weibull distribution are comparable to those obtained independently by API (API—American Petroleum Institute, 2007, "Interim Guidance on Hurricane Conditions in the Gulf of Mexico," API Bulletin No. 2INT-MET). However, the use of objective criteria to identify the optimal distribution suggests that the GEV estimates are to be preferred if the engineer wishes to emphasize the upper tail where extremes are likely to occur. The maximum increase in the SWH_{100} due to the 2004–2008 season is of the order of 0.9 m to 2.7 m (depending as the distribution). Information generated here is intended to supplement the design recommendations provided by API (American Petroleum Institute, 2007, "Interim Guidance on Hurricane Conditions in the Gulf of Mexico," API Bulletin No. 2INT-MET).
[DOI: 10.1115/1.4023205]

1 Introduction

Until recently, significant wave heights (SWHs) corresponding to the 100-year return period used for the design of various oil and gas facilities in the Gulf of Mexico (GOM) were of the order of 11 m (API [1]; Palao et al. [2]; Panchang et al. [3]). During the years 2004–2008, however, the GOM (shown in Fig. 1) experienced waves of unusual height relative to the "extreme" conditions. For instance, during Hurricane Ivan in 2004, SWH's of the order of nearly 16 m were recorded by a National Data Buoy Center (NDBC) buoy before it malfunctioned; and, SWHs as large as 17.9 m (corresponding to "maximum" wave heights of approximately 27.9 m) were recorded by Wang et al. [4], who suggest that even larger waves may have occurred. Comparably large (and at some locations, larger) wave heights, well in excess of the 100-year return period estimate, were recorded again during Hurricanes Katrina (Sept. 2005), Dennis (July 2005), Rita (Sept. 2005), and Ike (Sept. 2008). The extreme storm surge, wind, and wave conditions, which have been documented and analyzed in part by Hovis [5] (2005) and by Panchang and Li [6] (2006), caused extensive damage to the numerous oil and gas facilities in the Gulf of Mexico [7].

The National Data Buoy Center (NDBC) maintains eleven wave buoys in the GOM (Fig. 2) that provide wave data for time periods ranging between 7 and 33 years. Table 1 provides a summary of these data and includes the highest and second highest SWHs recorded at the buoy locations. When the maximum measured SWHs are associated with a recent storm, the name has been included. It is clear that, at seven of the buoy locations (42001, 42,003, 42,007, 42,019, 42,035, 42,039, and 42,040) maximum measurements for the 2004–2008 hurricane seasons are larger than previous maxima. While the differences are marginal at some of the buoy locations, they are substantial at three locations (42039, 42,040, and 42,007): the previous largest SWH recorded at these locations were 9.3 m (in 1998), 10.8 m (in 1998), and 4.9 m (2002), respectively. Although two of these locations have relatively short datasets, the differences are notable at the

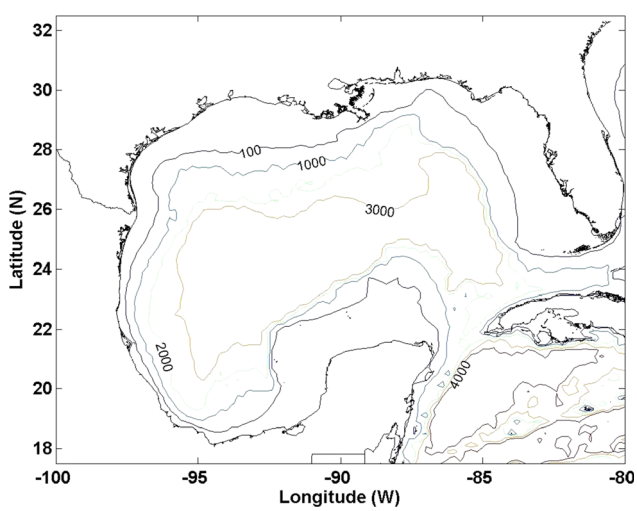

Fig. 1 Gulf of Mexico, map and bathymetry (m)

[1]Corresponding author.

Contributed by the Ocean, Offshore, and Arctic Engineering Division of ASME for publication in the Journal of Offshore Mechanics and Arctic Engineering. Manuscript received May 14, 2012; final manuscript received September 9, 2012; published online May 2, 2013. Assoc. Editor: Hideyuki Suzuki.

Copyright © 2013 by ASME

Downloaded From: http://offshoremechanics.asmedigitalcollection.asme.org/ on 03/12/2014 Terms of Use: http://asme.org/terms

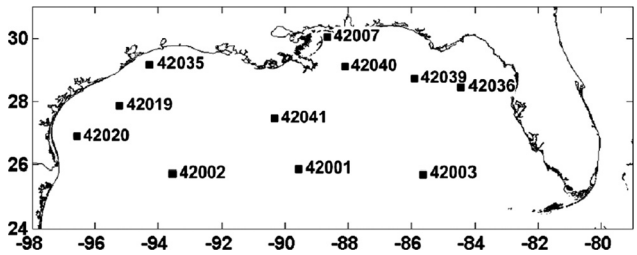

Fig. 2 Approximate locations of NDBC buoys in the Gulf of Mexico

locations of buoys 42,007 and 42,040; at the latter buoy location, extremely large differences (relative to previous maxima) were recorded during two events: Hurricanes Ivan and Katrina.

The measurements, summarized above, would suggest the possibility of an increasing trend in the SWHs in the GOM. Such trends in the wave climate are being increasingly reported. Wang et al. [8] used a variety of models and projected a 60–100 cm increase in the fall 20-year wave heights in the Norwegian Sea between 1990 and 2080; for the northeast Atlantic, they project a 5–35 cm increase in the mean winter wave heights in 2070–2099 relative to 1961–1990. Off the California coast, Graham [9] reported an increasing trend in the largest modeled SWHs of about 1.0–2.5 m for the 1949–1999 period. Examining buoy data, Komar and Allan [10] reported an increase of 1.7 cm/year off the east coast; and Ruggiero et al. [11] reported an increase of about 7.1 cm/year in the largest SWHs since the mid-seventies off the U.S. northwest coast. An increasing trend in the GOM, if one were to exist, could be of considerable import, given the enormity of the engineering enterprise in these waters. Trend estimates are needed for nonlinear approaches to extremal analyses and have been used; for example, by Warner and Tissot [12] and Obeysekera et al. [13] in the context of water levels off the GOM coast. Following the approach taken by Graham [9], this issue is examined for the GOM using several decades of (modeled) data.

As a result of the occurrence of the extremely large waves, the American Petroleum Institute (API) initiated efforts to reexamine the specification of design conditions for offshore structures in the GOM. These efforts, summarized by Berek et al. [14], were based on a combination of synthetic (hindcast) wind and wave information obtained with proprietary models and the Weibull distribution (with the peak over threshold method) for hurricanes that occurred prior to 2007. In some regions of the GOM, these new estimates indicate substantial increases in the 100-year (design) wave height and wind speed; relative to API's previous estimates, the maximum increase is as much as 6.4 m at a given location in the maximum wave height and 5 m/s in the wind speeds. According to API [1], the maximum estimated 100–year SWH (denoted by SWH_{100}) in the GOM was approximately 12 m, whereas the revised estimate is 15.8 m (Berek et al. [14]).

The magnitude of the increases and their implications for engineering call for a more comprehensive investigation of the issue, since the API calculations do not cover the entire Gulf and, more importantly, such extreme value estimates can be sensitive to both the data and to the statistical methods used to generate them. The importance of this was highlighted by the events associated with Hurricane Ike (2008), when SWH's that equaled or exceeded API's new SWH_{100} estimates were recorded at some locations. (As noted earlier, the API [15] study does not include storms after 2006.) In an effort to augment the work described in API [15], we revisit the problem by independently generating 51 years of detailed numerical simulation data and using multiple statistical methods. Additional estimates obtained here are intended to help the engineer make informed decisions and to assess the uncertainty associated with the results.

The quality of data is fundamentally important for metocean studies affecting risk-based design of offshore structures. Although measured data are probably the best source, individual measurement sites are widely distributed and the lengths of records are relatively short or discontinuous. As a result, measured data are usually insufficient to characterize waves over large ocean areas. An alternative method of data development is to use numerical models to calculate the wave conditions based on measured or modeled winds. This method of developing wave data for subsequent probabilistic or climatological analyses has been used; for example, by Pontes et al. [16] to develop a nearshore atlas for wave energy calculations in Portugal, Millar et al. [17] to examine the impacts of wave energy farms off the UK coast, Panchang et al. [18] for aquaculture applications, and Cieślikiewicz and Paplińska-Swerpel [19] to develop a 44-year wave hindcast in the Baltic.

Yet, synthetic data are potentially vulnerable to many modeling-related errors (e.g., Rogers et al. [20]; Cardone et al. [21], and probabilities can be affected by the choice of events chosen for modeling. Berek et al. [14] have generated the data by hindcasting "select" storms for the period 1950–2006 using proprietary modeling tools, and while some details of their error analysis are available (e.g., Forristall [22]) provides an assessment of their models for four storms), the multifarious nature of the data generation process demands the use of alternative tools and models. Here we have used alternative numerical models to create a continuous 51-year (1958–2008) hindcast. Further, we have used all publicly-available wind and wave data to validate the model results, to the maximum extent possible, and to make appropriate adjustments to both the models and to the results prior to preparing a final dataset for statistical analysis. In particular, we have used a modified parametric wind field model (Jeong et al. [23]) that includes improvements based upon a comparison of such models against "HWIND" data (Powell et al. [24]) for a large number of storms covering nearly 30 years. Also, nearly 35 years of wave buoy data were used to validate not only individual storm simulations but also the SWH_{100} estimates.

In addition to data reliability, the choice of the dataset itself is important for characterizing extreme events (e.g., Xu and Huang

Table 1 Wave data description in the Gulf of Mexico

Buoy	Data duration (year)	Depth (m)	Maximum SWH (m)		2nd largest SWH (m)	
42001	1976–2008 (33)	3246.0	11.63	(Sept. 2005)–Rita	11.2	(Oct. 2002)
42002	1976–2008 (33)	3566.2	9.70	(Sept. 1988)	8.4	(Nov. 1980)
42003	1977–2008 (32)	3233.0	11.04	(Sept. 2004)–Ivan	10.7	(Nov. 1985)
42007	1981–2008 (28)	14.0	9.09	(Sept. 2004)–Ivan	5.64	(Aug. 2005)–Katrina
42019	1990–2008 (19)	82.3	6.3	(Sept. 2008)–Ike	5.92	(Sept. 2005)–Rita
42020	1990–2008 (19)	88.1	8.20	(Aug. 1999)	6.79	(Oct. 1996)
42035	1993–2008 (16)	13.7	7.1	(Sept. 2008)–Ike	4.7	(Sept. 2005)–Rita
42036	1994–2008 (15)	54.5	8.60	(Oct. 1995)	6.9	(Jan. 1994)
42039	1995–2008 (14)	291.4	12.05	(Sept. 2004)–Ivan	10.6	(July 2005)–Dennis
42040	1995–2008 (14)	443.6	16.91	(Aug. 2005)–Katrina	15.96	(Sept. 2004)–Ivan
42041	1999–2005 (7)	1055.7	12.31	(Oct. 2002)	8.56	(Sept. 2004)–Ivan

Downloaded From: http://offshoremechanics.asmedigitalcollection.asme.org/ on 03/12/2014 Terms of Use: http://asme.org/terms

[25]). Also, the n-year return period estimates can be highly sensitive to the chosen statistical model, and to the "threshold" in the peak-over-threshold method that is commonly used for extreme estimation (Van Vledder et al. [26]). While Berek et al. [14] have chosen, a priori, the Weibull distribution, the question of whether this is the best distribution has not been addressed, nor has the sensitivity of their results to the threshold.

In view of these considerations, a comprehensive study was conducted for estimating the variability inherent in the SWH_{100} estimates resulting from the use of different sets of data and different statistical methods for the entire Gulf of Mexico. In particular, we are concerned with the following questions that can influence design choices:

(1) How do SWH_{100} values obtained by modeling compare with those obtained from buoy data? What is the effect of modeling errors on the SWH_{100}? What is the effect of data length on the estimates? These issues are of concern since some estimates in the past (e.g., Panchang and Li [6]) have been obtained using buoy data which have the benefit of being free of modeling-related errors and can be used either for design (and are used here for validating modeled estimates). Buoy data are available for varying time periods, whereas model results were developed here for 51 years.
(2) What is the variability associated with the choice of other distributions? Three commonly used extreme value distribution functions (Gumbel, Weibull, and generalized extreme value) were evaluated to select the optimal one for extremal estimation. Further, selection of the most appropriate model for different areas is usually a difficult and subjective problem. Recently Li et al. [27] provided robust and quantitative means for identifying the most appropriate model based on the engineer's preference, rather than limiting oneself to any preselected model.
(3) Are there trends in the wave climate in the GOM? What is the effect of the recent (2004–2008) extreme hurricane season on the estimates of SWH_{100}?

The paper is organized as follows. Section 2 provides details about available wind and wave information in the GOM. It also examines the performance of three commonly used parametric wind models when applied to recent storms and briefly describes adjustments to the Rankine vortex model to obtain more reliable hurricane windfields (Jeong et al. [23]). The wave modeling methodology used to obtain wave characteristics at an appropriately fine resolution, modeling errors, adjustments, and validation of the calculated wave heights are described in Sec. 3. A portion of the results, relating to trends, is presented in Sec. 4. Section 5 summarizes the statistical methods used here for extreme wave height estimation. Validation of the statistical estimates using model data and buoy data is presented in Sec. 6; this involves limiting the model dataset to the length of the buoy data. In Sec. 7, the full 51 years of model data are used to obtain SWH_{100}, using the three distributions and the behavior of each is examined. This helps identify the most appropriate SWH_{100} estimate at each grid point. Section 8 summarizes the results of this study.

2 Modeling of Wind Fields

Three sources of wind fields, described in Table 2, are available to force a wave model. For the generation of estimates corresponding to a n-year event, a rule of thumb (Borgman [28]) states that the dataset should preferably be at least n/3 years long; this precludes the exclusive use of two ("NCEP" and "HWIND") of the three sources in Table 2 for the development of SWH_{100} estimates. And, while the "Reanalysis" dataset (Kalnaya et al. [29]) is available for a longer time duration and possesses sufficient temporal resolution (12 mins) and has hence been used for other large ocean basin wave studies (e.g., Music and Nickovic [30]; Cieślikiewicz and Paplińska-Swerpel [19]), its spatial resolution has been found to be too coarse for simulating the spatial details of hurricane waves (Jeong et al. [23]).

An alternative is to use "parametric models" to reconstruct the wind fields on the basis of a limited set of hurricane parameters. A hurricane dataset (HURDAT) pertaining to a limited set of storm parameters developed by the NOAA from 1851 to present (Jeong et al. [23]). However, the dataset is substantially detailed only for the post-1950 period. This dataset provides information at 6-hour intervals, information such as the location of the storm center, storm direction (θ_s), storm speed (V_s), maximum wind speed (V_m), and storm central pressure (P_c). Details are provided in Jeong et al. [23], and because the parametric models were used in this work, a brief summary is provided below.

We considered three commonly-used parametric models, viz. the Rankine Vortex (RV) model, the SLOSH model, and the Holland model (with asymmetries; see MacAfee and Pearson [31] for details) to obtain the wind speed $V(x,y)$ as a function of HURDAT parameters V_m and P_c and also of other model-calculated quantities such as radius to maximum wind (R_m) and sea level pressure at the last closed isobar (P_n). The models were applied to 56 HURDAT snapshots covering a wide range of hurricane development phases/levels. The results, documented in Jeong et al. [23], indicate that the models frequently produced considerable mismatch in velocity contours relative to the HWIND data. An example, using the RV model, is shown in Figs. 3(*a*)–3(*c*) for Hurricane Ike (1998). Wind speed errors are as large as 15 m/s; similar errors were encountered with the other two wind models. Jeong et al. [23] found that for Hurricane Katrina, the RV model winds led to an underestimate of the modeled wave heights by nearly 5 m at the peak of the storm.

Other researchers (e.g., Xie et al. [32], MacAfee and Pearson [31]) have also noted discrepancies between parametric wind models and data, and made adjustments to suit individual cases or regions. For example, Xie et al. [32] made adjustments to the Holland model based on an analysis of four mid-Atlantic hurricanes. For the GOM Jeong et al. [23] made adjustments to the RV model, using observed differences between modeled and measured data to develop empirical correction factors to modify the RV model.

While the reader is referred to Jeong et al. [23] for details of the modifications as well as validation, by way of example, we demonstrate in Fig. 3(*c*) the improvement obtained with the modified RV model as regards wind speed contours. The wave fields resulting from the two wind fields are shown in Figs. 3(*d*) and 3(*e*). For both wind and wave fields, although the maximum values are largely the same, the spatial patterns are different, leading to a maximum difference of about 3.4 m in SWH estimates at some locations. Since such large differences have the potential to affect extreme wave height statistics, the modified RV wind model was used for modeling the wave-fields.

Table 2 Windfield datasets

	NCEP	HWIND	Reanalysis wind
Source	Numerical model	Measured data	Numerical & available data
Resolution	$0.25° \times 0.25°$	$6\,km \times 6\,km$	$2.5° \times 2.5°$
Availability	1999–present	1994–present	1948–present
References	http://polar.ncep.noaa.gov/waves/index2.shtml?	Powell et al. [24]	Kalnaya et al. [29]

Downloaded From: http://offshoremechanics.asmedigitalcollection.asme.org/ on 03/12/2014 Terms of Use: http://asme.org/terms

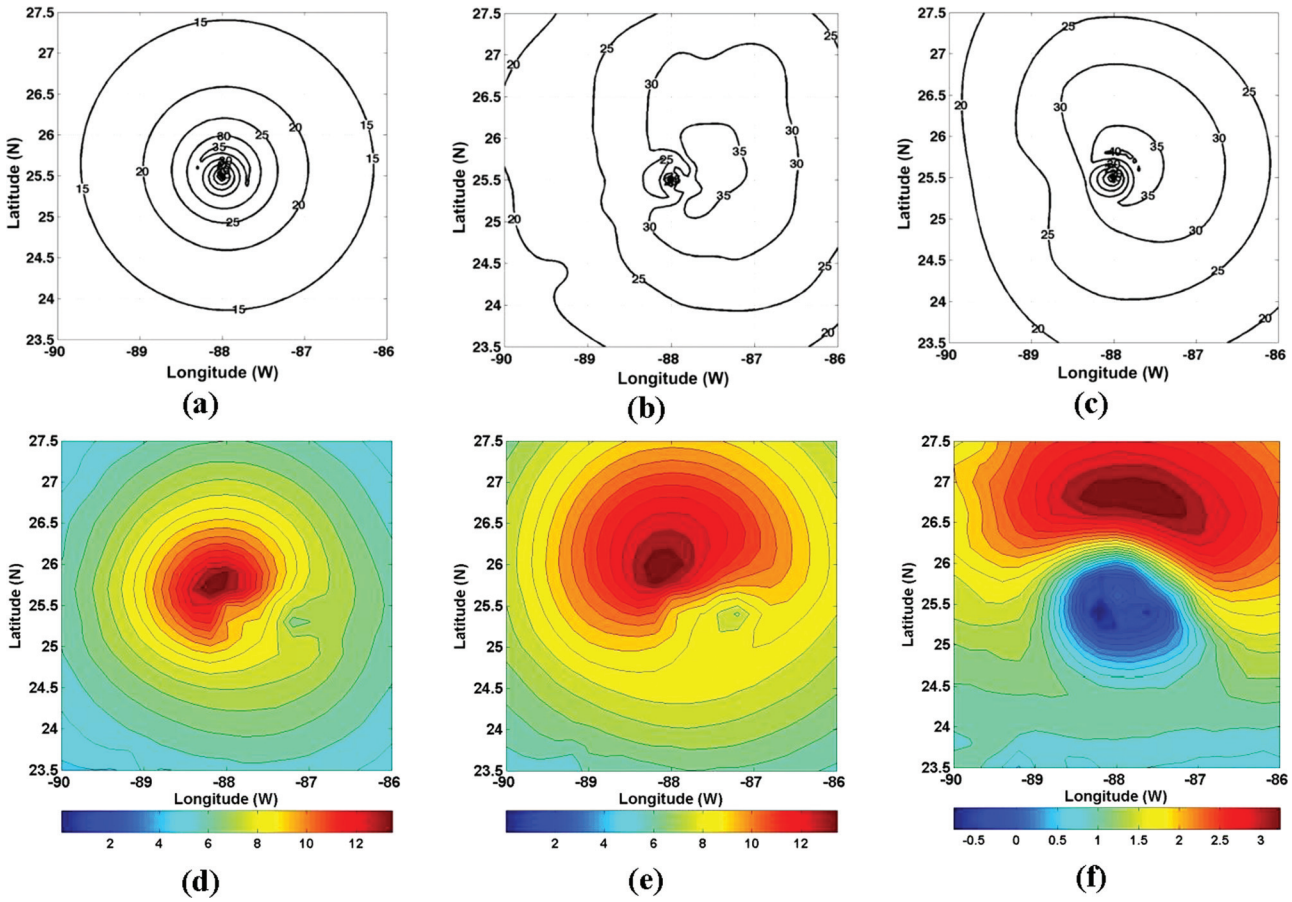

Fig. 3 Wind speeds and SWH's during Hurricane Ike (at 1200 UTC 9 Sept. 2008): (*a*) RV-model wind, (*b*) H*Wind, (*c*) modified RV-model wind, (*d*) SWH (m) using RV-model wind, (*e*) SWH (m) using modified RV-model wind, (*f*) the difference SWH (m) between (*d*) and (*e*)

3 Modeling of Wave-Fields

Wave data for the GOM are in fact developed by Texas Coastal Management Program (NOAA), using the model WAVEWATCH, as part of a large-scale simulation for the entire western North Atlantic, at a grid resolution of about (0.25°). Since this is insufficient for representing the intricacies of hurricane conditions, NOAA developed the "North Atlantic Hurricane" model but results are available only from 2000. Hindcasting with other methods is thus needed to provide data for extreme wave estimation for long return periods.

Toward that end, we used the third-generation wave-prediction model SWAN (Booij et al. [33]; Ris et al. [34]), which is based on the spectral action balance equation and includes the total rate of change of wave action, frequency shift and refraction induced by depth and currents the effects of generation, dissipation (due to breaking, bottom-friction, and white-capping), and nonlinear wave-wave interactions. Reflections and diffraction are incorporated in an approximate manner (Booij et al. [35]). Spectral or parametric wave input conditions may be specified along the boundaries. The model has been widely used and validated by several investigators (e.g., Booij et al. [33]; Zubier et al. [36]; Chen et al. [37]; Singhal et al. [38]).

A grid covering the entire Gulf of Mexico from 18°N to 32°N and from 80°W to 100°W at a spatial resolution of $0.2° \times 0.2°$ (101×76 grid points) was developed. The bathymetry, obtained from the National Geodetic Data Center, had a resolution of 2 mins (601×451 grid points). The model was run with 576 discrete spectral components ($\Delta\theta = 15°$ and Δf varying between 0.04 to 0.4 Hz with a logarithmic increment).

As noted earlier, the spatial resolution of the reanalysis windfield was found to impede the modeling of the spatial details of hurricane winds. The modified RV model winds were therefore used to replace the reanalysis winds in the hurricane area covering a $4° \times 4°$ region at a resolution of $0.05° \times 0.05°$. However, the benefits of incorporating "background" wind fields (viz., the wind fields outside the hurricane and also the wind fields that existed before the onset of the hurricane) have been indicated by Liu et al. [39]. Therefore we constructed a composite wind field (Fig. 4) by

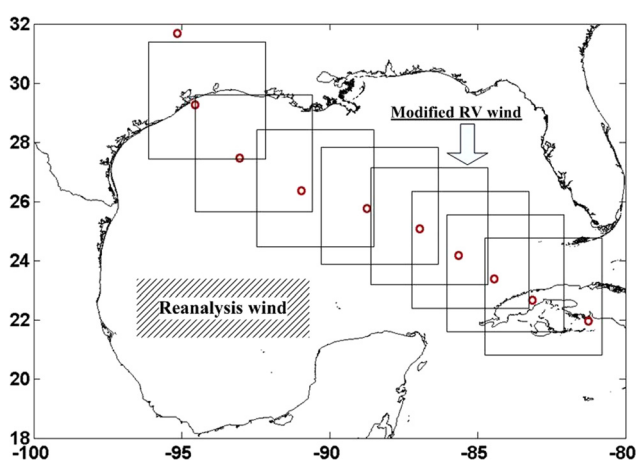

Fig. 4 Integration of windfields

Downloaded From: http://offshoremechanics.asmedigitalcollection.asme.org/ on 03/12/2014 Terms of Use: http://asme.org/terms

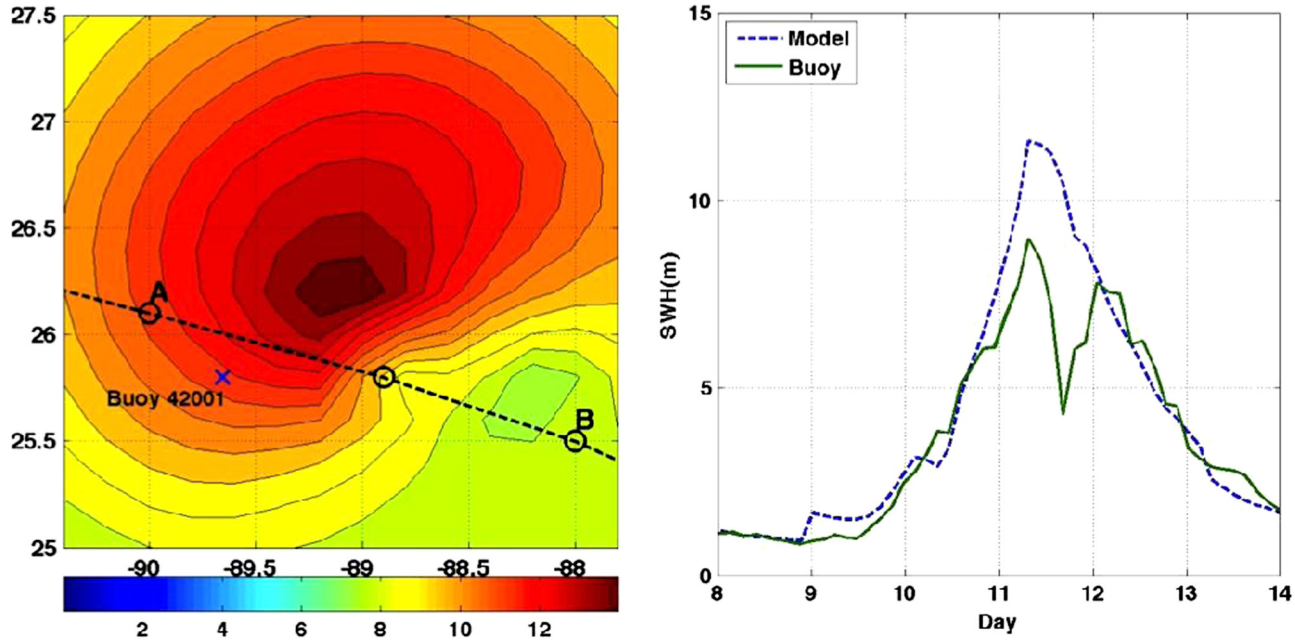

Fig. 5 SWH contour (*a*) and SWH comparison at buoy 42,001(*b*)

merging the parametric model winds with the reanalysis winds (the latter are interpolated onto a 0.05° grid).

3.1 Basic Results: Individual Storms. Even with the modified RV model winds, some difficulties remain while modeling the hurricanes. The HURDAT dataset provides the location of the storm center at 6-hour intervals. Here we have connected these locations (denoted by (*a*) and (*b*) in Fig. 5) by a straight line, which is assumed to be the storm track, and simulations are made for intermediate times by placing the storm center on this line by interpolation. This leads to problems in some instances. For example, Fig. 5 shows that, during Hurricane Ike, the simulations did not successfully capture the two peaks seen in the SWH data at the location of buoy 42,001, the occurrence of which indicates that the buoy is close to the actual storm track (possibly with the eye of the storm passing in the vicinity). However, the assumption of line AB as the assumed storm track yields a simulation containing only one peak, and hence substantial errors in SWHs, at the buoy location. Thus, the actual storm track could be off by as much 30 km (based on this example).

To address the problem of storm track uncertainty, Heideman and Mitchell [40] resorted to a technique called "grid point pooling," which involves collecting estimates from several points in a preselected area (see also Jonathan and Ewans [41]), and then using them for statistical analysis. However, as they acknowledge, this violates the requirement of statistical independence because each storm is included multiple times. They recommended some general guidelines to ameliorate this issue, including a selection of spatially homogeneous regions, which is subjective and difficult.

Since the SWHs show considerable variability in the vicinity of the storm center, we applied a smoothing to the simulated SWHs by using model data from 2 grid points on all four sides of a given point (i.e., a nine-point smoothing). Sample results are shown in Figs. 6 and 7 for Hurricane Ivan. Comparisons with data, shown in Fig. 7, indicate that the model simulations are fairly realistic, and also show the occurrence of SWHs larger than 10 m. At buoy 42,007, though, the measured SWHs are larger than model data. Several factors could adversely affect the modeling effort and the comparisons. The first is the storm surge effect (i.e., wind-induced water level changes and surface currents), which can modify the waves in shallow water. This effect is not included in the simulation. A more likely source of errors may be due to inaccuracies in the wind-fields in the near-shore areas arising from the presence of islands (near buoy 42,007). Other possible reasons for modeling errors are inaccurate representations of the bathymetry (including subgrid-scale topographic features) and model limitations (e.g., Rogers et al. [20]). There can also be data problems. Bender et al. [42] reported possible errors in SWH measurements for buoy 42,007 by approximately 11% during Hurricane Katrina possibly due to swell in shallow water, heeling of the buoy caused by winds and currents, and a failure to tilt-correct the accelerometer data. Unfortunately, no generalized means to assess the NDBC buoy data and to correct them are readily available.

Additional comparisons of model SWHs and historical data are shown in Fig. 8. The data were collected from a fixed platform near Louisiana during Hurricane Camille (1969), which passed within 23 km of the platform. These data are older than all the NDBC data. The measured maximum SWH is 13.45 m and modeled SWH is 14.65 m [43]. Note that data are available only for a part of the hurricane. The comparisons are reasonable, especially

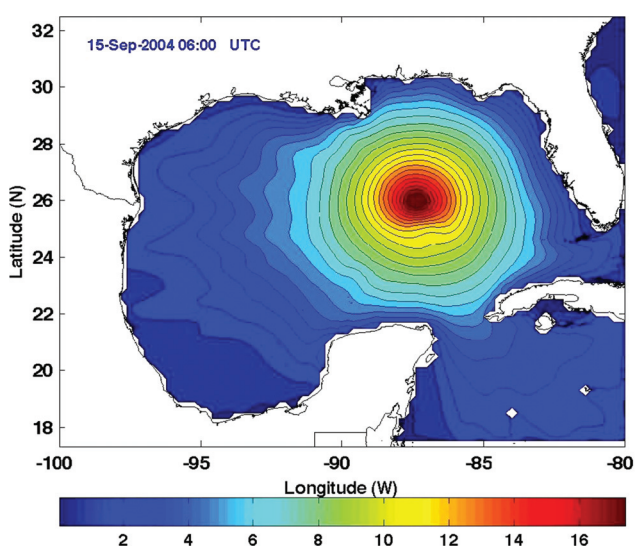

Fig. 6 Modeled SWHs for Hurricane Ivan

Downloaded From: http://offshoremechanics.asmedigitalcollection.asme.org/ on 03/12/2014 Terms of Use: http://asme.org/terms

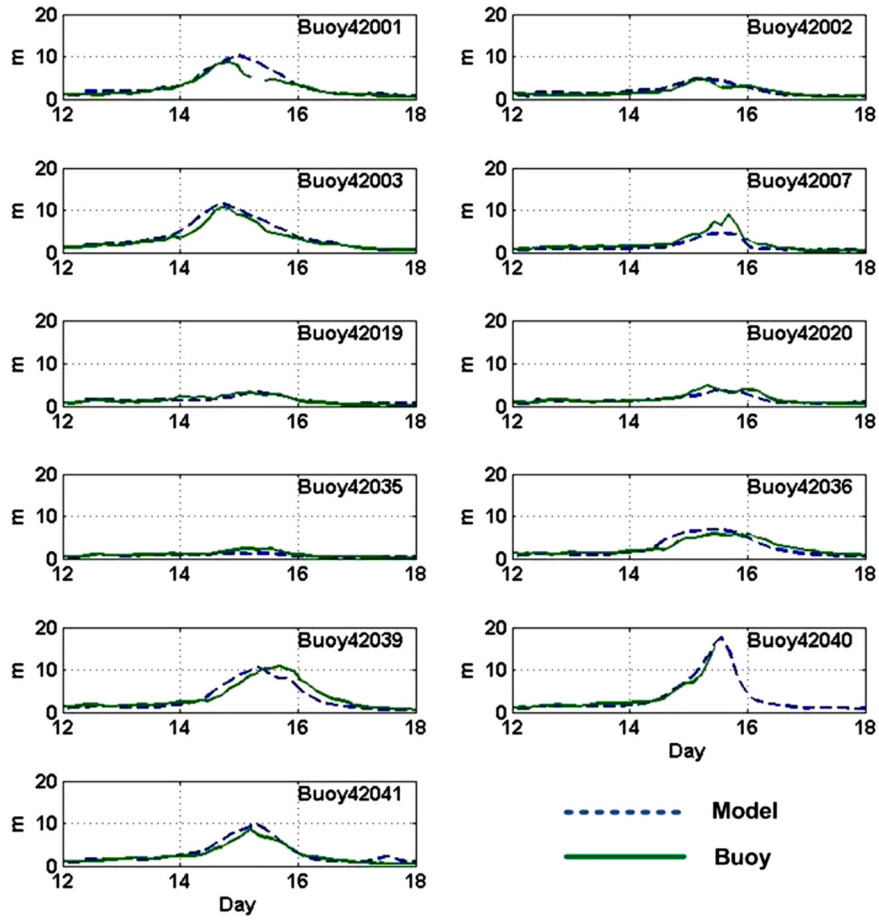

Fig. 7 SWH comparisons

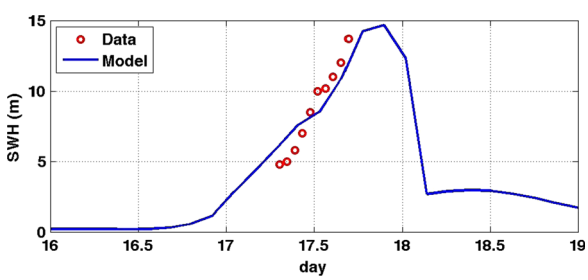

Fig. 8 SWH comparison during Hurricane Camille (Aug. 1969)

Table 3 Maximum SWH's along Texas coast during Hurricane Ike

Gage	Gauge max. SWH (m)	Modeled max. SWH (m)
R	4.5	3.99
S	2.9	3.36
U	4.9	4.6
V	4.5	4.85
W	5.1	5.3
X	5.6	6.1
Y	4.8	5.3
Z	5.6	5.55

if one takes the storm track uncertainty into consideration. Finally, turning to coastal regions, we show in Table 3 a comparison of modeled SWHs with data from the eight gauges deployed by Kennedy et al. [44] during Hurricane Ike. The gauges, denoted by the letters R through Z, were located along the Texas coast northwards from Corpus Christi in water depths between 8.7 m and 15.8 m. Again, the comparison is reasonable (generally the differences between the modeled SWHs and the data are less than 0.5 m).

3.2 Generation of SWH Database. For the 1958–2008 period, HURDAT snapshots are available for 145 hurricanes in the GOM. However, the data are incomplete for 18 hurricanes; therefore only the remaining 127 hurricanes were included. The modified RV model was used to reconstruct the hurricane windfields, which, as noted earlier, were supplemented with the reanalysis winds; the resulting wave conditions modeled as described in preceding paragraphs. Since it is the maxima in specific time intervals that influence the extreme wave statistics, it is necessary to assess the quality of such maxima. Here, we use the monthly maxima at the location of the eleven buoys for assessing the simulations. Figure 9 shows a comparison involving a total of 2760 pairs. It must be noted that the comparison involves a small subset of the overall model results, since the buoy data-lengths are much smaller than the overall modeling period and there were instances where the buoy stopped recording. For the comparison, model data from the grid point closest to the buoy has been used. Figure 9(*a*) shows that most of the model data and buoy data are fairly close to the slope-one line (slope of the best-fit line is ~0.82), indicating that the model data are, for the most part, reasonable surrogates and can be used for further (statistical) analyses. However, closer examination reveals that in the case of larger wave heights the predicted SWHs appear to be larger than data.

Since larger wave heights are of importance in the extreme value statistics, we separated the 2760 points into two sets, those larger than 7 m and those smaller than 7 m and the best fit line obtained for each (Fig. 10). The formula from the best-fit line can

Downloaded From: http://offshoremechanics.asmedigitalcollection.asme.org/ on 03/12/2014 Terms of Use: http://asme.org/terms

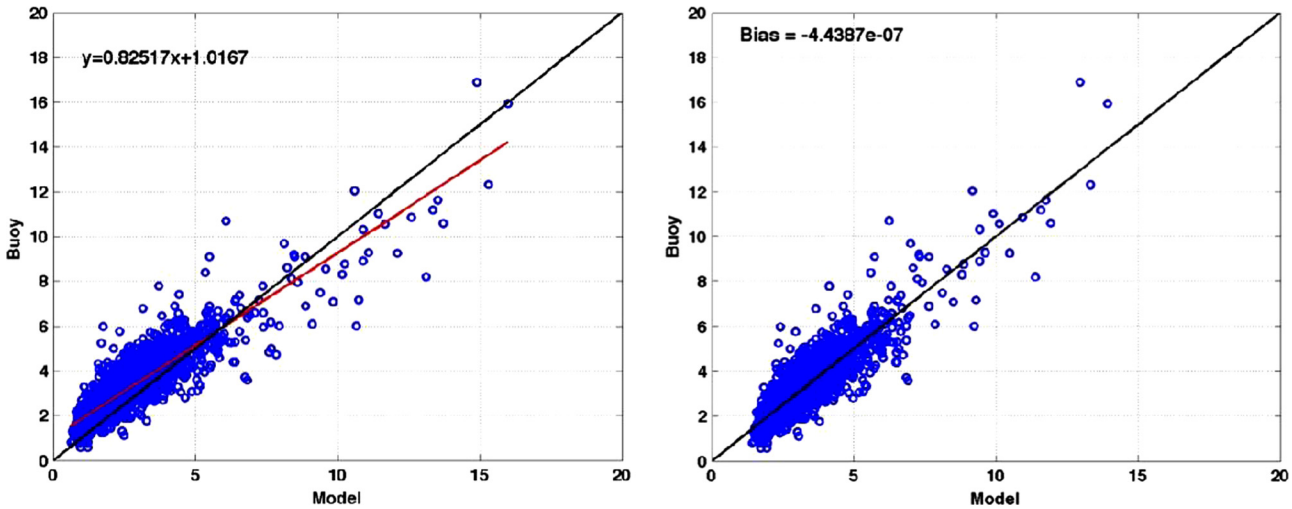

Fig. 9 Comparison of monthly maxima for the eleven NDBC buoys

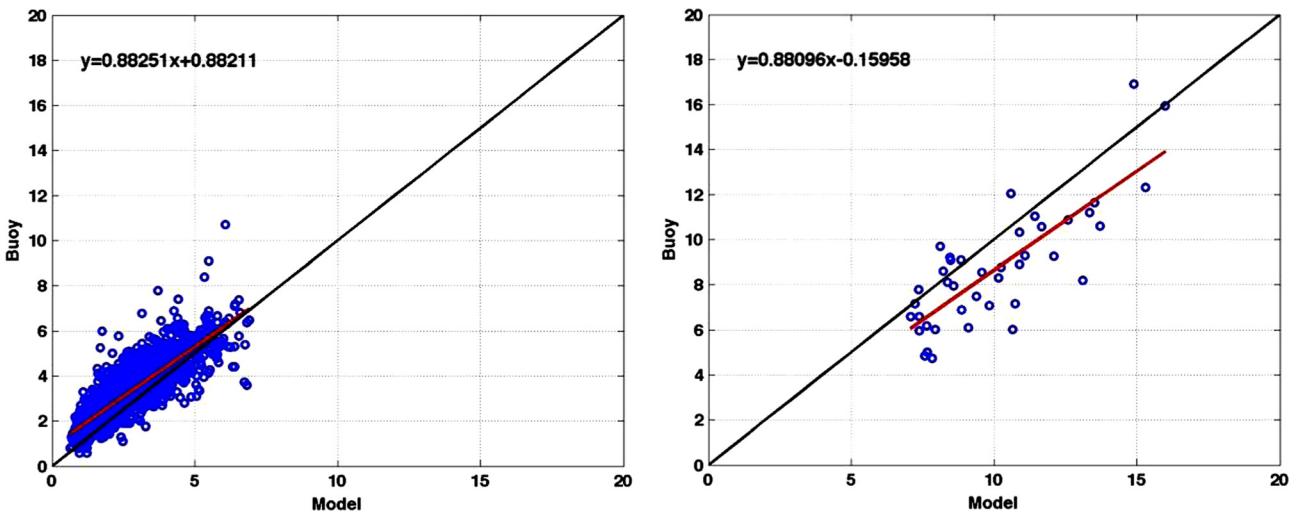

Fig. 10 Best-fit lines for two groups of monthly maxima

be used to modify the simulated SWHs in order to improve the surrogate dataset. The modified results are shown in Fig. 9(*b*) for all eleven buoy locations and the comparison appears fairly reasonable. As a result, the correction was applied to all modeled results.

4 Trends in the Wave Climate

Using the simulations for the pre-2004 period and for the period including the 2004–2008 hurricane season, the maximum SWH obtained from the simulations at each of the 7676 grid points was determined. Figure 11 shows the number of times the SWH exceeded 10 m in the Gulf of Mexico; the frequency and spatial extent of these large waves clearly increased during 2004–2008. The maximum number of events exceeding 10 m in SWH during first 46 years is 8, but is of the order of 12 or more the last four years (2004–2008). The largest modeled SWHs occurred in 1969 (Hurricane Camille), with a simulated value of approximately 18 m in the offshore areas (27°5′N, 87°8′W).

As mentioned in Sec. 1, several researchers have noted an increasing trend in the wave climate in various parts of the Atlantic and the Pacific oceans. Identification of such trends is important for establishing design criteria based on nonlinear (i.e., time-dependent) statistical models (e.g., Wang et al. [8]; Jeong and Panchang [45]; Ruggiero et al. [11]). For the GOM, we plotted the annual SWH maxima as a function of time for each grid point and determined the slope of the best-fit line. The results, summarized in Fig. 12, indicate that there is a decreasing trend in the western half of the GOM (spatial average = −1.6 cm/year), while the eastern half shows an increasing trend (spatial average = +2.05 cm/year). The maximum increasing trend in the eastern half is of the order of 5.6 cm/year, comparable to the estimates reported by Graham [9] and Ruggiero et al. [11] for the U.S. west coast for the Pacific. If only data after the mid-seventies is examined, the maximum trend estimates are approximately 4.8 cm/year (for 1975–2008) and 7.95 cm/year (for 1976–2008); and if the recent extreme hurricane season is excluded, they are 1.77 cm/year (for 1975–2003) and 5.90 cm/year (for 1975–2003).

5 Statistical Methods

Estimating the extreme wave statistics at each location is usually done by fitting a distribution to the extremes in successive time intervals and then using the distribution to estimate the probability of occurrence associated with a specified SWH. The most common distributions appear to be the Gumbel, the Weibull, and (more recently) the generalized extreme value (GEV) distributions (e.g., Xu and Huang [25]; Panchang et al. [18,3]; Neelamani et al. [46]; Perez et al. [47]; FEMA [48]; Pontes et al. [16]). The parameters associated with these distributions were estimated for a given

Downloaded From: http://offshoremechanics.asmedigitalcollection.asme.org/ on 03/12/2014 Terms of Use: http://asme.org/terms

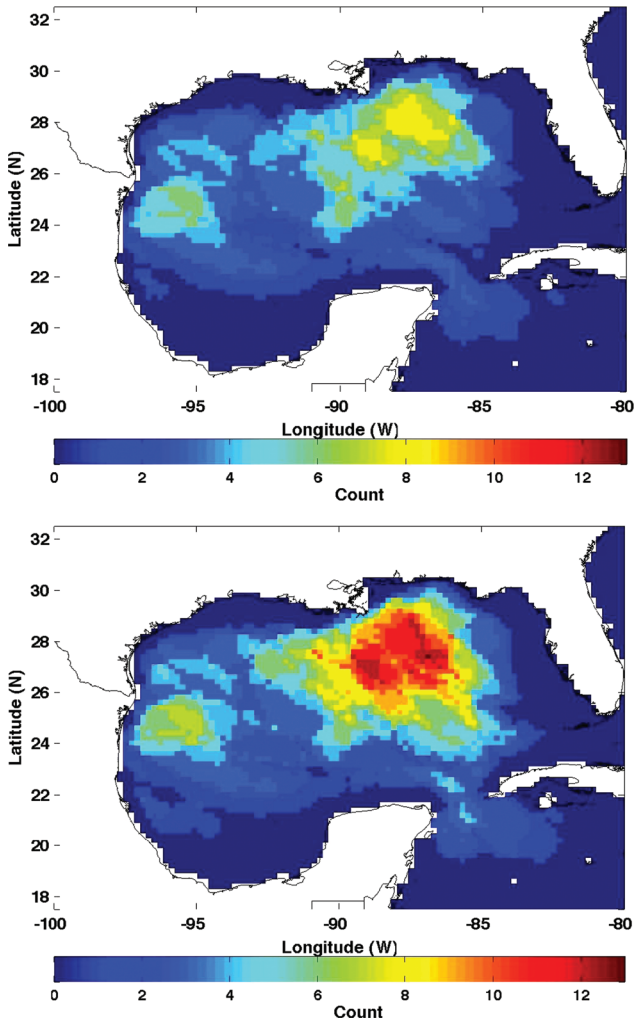

Fig. 11 Number of times SWH > 10 m: 1958–2003 (*a*), and 1958–2008 (*b*)

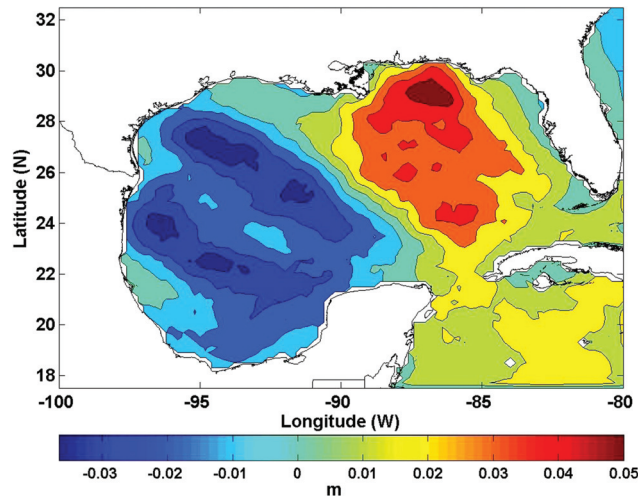

Fig. 12 Trend distribution

set of data (say $x_1, x_2, x_3, \ldots, x_n$) by the method of maximum likelihood. The probability associated with a specified "recurrence interval" or the "return period" N (in years) is

$$P(\mathrm{SWH} < \mathrm{SWH_N}) = 1 - \frac{1}{SN}$$

(where S is the number of data points per year and $\mathrm{SWH_N}$ is the SWH associated with a return period of N years), and the corresponding $\mathrm{SWH_N}$ is determined by equating this probability to the cumulative density function. As stated earlier, a rule of thumb (Borgman [28]) permits extrapolation to duration that is approximately three times as long as the length of the data. To create the dataset ($x_1, x_2, x_3, \ldots, x_n$) we have followed the classical approach which involves the use of a subset corresponding to the annual maxima (e.g., Carter and Challenor [49]); this can generally be expected meet to the requirement of the extremal distributions that the extremes be drawn from samples (in this case, annual data) which belong to the same population. We did not model the effects of directionality or seasonality as described by Jonathan et al. [50] and Jonathan and Ewans [41,51] since the expected improvements are still a matter of debate (Mackay et al. [52]; Jonathan and Ewans [53].

As to the choice of distribution, most engineering studies confine themselves to a preselected distribution (e.g., Neelamani et al. [45]; Berek et al. [14]); if multiple models are used, a number of subjective measures (e.g., Petrauskas and Aagaard [54]) are used to identify the preferred model. Not only is this tedious, but this also constrains one to the chosen model when comparing multiple time-frames. We follow recent developments by Li et al. [27] who have provided more robust and quantitative ways based on the jackknife and the bootstrap resampling methods along with an error norm for such identification. Thus, the most appropriate model can be selected by the engineer, rather than limiting oneself to any preselected model.

In the bootstrap method, a large number of alternative but equally plausible datasets are created by resampling the original dataset. The Jackknife method can also be used to create resampled datasets, but the bootstrap method is selected because the degree of randomness in the bootstrap resampling is apparently greater and the stability of the optimized parameters has been rigorously tested by Li et al. [27]. The weighted error norms of the maximum likelihood optimizations for each of the three cumulative density functions are calculated as the average of $K = 500$ bootstrap replicates based on the difference Δ between the empirical and the model probabilities (Li et al. [27]):

$$E\langle \Delta_i(\bar{Q}_j)\rangle = E\left\langle \max_{1\le i\le m}\left|\left[\frac{i}{m+1}\right]^h - G_{\bar{Q}_i}(r_{ij})^h\right|\right\rangle$$

where E stands for the expected value, $\bar{Q}$ is optimized parameter, $G_{\bar{Q}}$ is the cumulative density function under consideration, $r_1, r_2, \ldots, r_m$ are the ordered data X in increasing magnitude, and $j = 1, 2, \ldots, K$ represents the individual sample number.

The distribution with the smallest error norm is to be preferred. The parameter h controls the emphasis that we place on different parts of the data while fitting the distribution to the data. When $h = 1$, both the lower tail and the upper tail are equally important. For $h < 1$, emphasis is placed on the lower tail, while $h > 1$ emphasizes the upper tail where 'extreme' events occur. Computations using these methods were made at all grid points in the GOM and the preferred distributions based on the error norm are discussed in Sec. 7.

6 Application of Probability Distributions to Model Data and Buoy Data: Validation

Models are an effective way to create a long-term (51 years in this case) grid-based database for extreme wave height estimation, allowing the creation of a dataset consisting of annual maxima required in the classical method of extremal analysis. However, even when using the best models, errors are inevitable, as seen in Sec. 3, and generally the numerical results are checked against data, when possible, for individual events. The cumulative effects

Downloaded From: http://offshoremechanics.asmedigitalcollection.asme.org/ on 03/12/2014 Terms of Use: http://asme.org/terms

Table 4 Summary of NDBC buoy data

Buoy	Total data available	Missing data	Comments
42001	1976–2008 (33)	1976–1978 (Poor quality) 2007 (Jan.–Feb.)	NA
40002	1976–2008 (33)	1976 (Jan.–Sept.) 1977 (Aug.–Sept.) 1978 (Aug.)–1979 (Nov.) 1980 (Aug.) 1999 (Jan.–Feb.) 2001 (Jan.–Aug.) 2005 (July)	Three large SWHs (~10 m) are missing (1977, 1980, and 2005). At other times, when data are missing, model results indicate mostly small SWH's, but sometimes of the order of 5 m.
42003	1977–2008 (32)	1977 (Jan.–Jun.) 1986 (Nov.)–1987 (Apr.) 1987 (Dec.)–1988 (Apr.) 1994 (Sept.)–1995 (Jan.) 1996 (Sept.)–1997 (May) 2005 (Aug.–Sept.) 2008 (Aug.–Nov.)	One large SWH (~10 m) is missing (2008). At other times, when data are missing, model results indicate mostly small SWH's, but sometimes of the order of 5 m.
42007	1981–2008 (28)	1981 (Oct.)–1983 (Jan.) 1983 (Apr.–Dec.) 1987 (Jan.–Apr.) 1990 (Aug.)–1996 (Sept.)	When data are missing, model results indicated fairly small SWH's (< 3.5 m).
42019	1990–2008 (19)	1990 (Jan.–May) 2000 (Jan.–Jun.)	NA
42020	1990–2008 (19)	1990 (Jan.–May) 1993 (Aug.–Nov.) 1997 (Feb.–Oct.)	NA
42035	1993–2008 (16)	NA	~40 km buoy drift during Hurricane Ike.
42036	1994–2008 (15)	2005 (July) 2007 (Feb.–Sept.)	One large SWH (~10 m) is missing (2005).
42039	1995–2008 (14)	1995 (all)	Annual maximum data from 1996 are used.
42040	1995–2008 (14)	1995 (Jan.–Nov.)	
42041	1999–2005 (7)	1999 (Jan.–Nov.) 2001 (March)–2002 (April) Disestablished after 2005 (April)	Almost half the data are missing.

of the errors on the estimated SWH_{100} are rarely examined. Of course, if the overall modeled dataset is long, one can expect the effect of individual modeling errors (i.e., inaccurate data) on SWH_{100} to be small; and if the dataset is short, or if even a few errors are very large, one can expect a greater impact on the estimated SWH_{100}. However, the effect of the errors on the estimated SWH_{100} must be quantified before proceeding to an eventual application of the statistical models to the full modeled dataset.

Table 5 Estimated SWH_{100} (m)

				(*a*) Before (2004)			(*b*) Including 2004–2008		
Buoy no.	Data	Δ (km)	No. of year	Gumbel	Weibull	GEV	Gumbel	Weibull	GEV
42001	Buoy	20	28/33	10.62	10.95	12.84	12.64	12.32	14.74
	Model			11.65	12.63	14.2	12.90	14.31	16.1
42002	Buoy	12.4	28/33	10.36	9.49	10.47	9.80	9.12	9.82
	Model			12.11	12.45	14.56	11.95	12.76	14.25
42003	Buoy	16.1	27/32	10.64	11.24	12.62	12.44	12.43	14.25
	Model			12.27	13.24	15.03	13.44	14.92	16.09
42007	Buoy	3.6	23/28	5.75	7.02	5.78	7.61	10.4	10.53
	Model			6.71	8.2	8.07	7.16	8.0	7.92
42019	Buoy	5.4	14/19	7.18	6.20	6.26	7.25	6.80	6.88
	Model			8.52	8.98	10.0	8.51	9.30	9.71
42020	Buoy	12.8	14/19	8.05	9.40	10.90	9.02	9.94	10.47
	Model			12.37	11.26	14.83	12.59	12.90	17.19
	Model*			8.03	8.1	10.0	9.9	10.5	13.5
42035	Buoy	7.7	11/16	5.94	7.55	6.59	6.76	7.53	7.44
	Model			5.37	5.67	6.4	6.24	6.75	7.39
42036	Buoy	9.2	10/15	9.9	11.52	10.28	9.57	8.90	8.84
	Model			9.21	10.77	9.36	10.8	13.08	10.78
42039	Buoy	10.1	8/13	11.0	11.9	13.01	14.49	19.2	17.8
	Model			11.3	12.39	13.53	14.15	19.24	17.3
42040	Buoy	9.8	8/13	13.2	16.35	19.45	21.9	31.2	31.8
	Model			13.02	14.85	19.1	18.48	23.45	24.56

Downloaded From: http://offshoremechanics.asmedigitalcollection.asme.org/ on 03/12/2014 Terms of Use: http://asme.org/terms

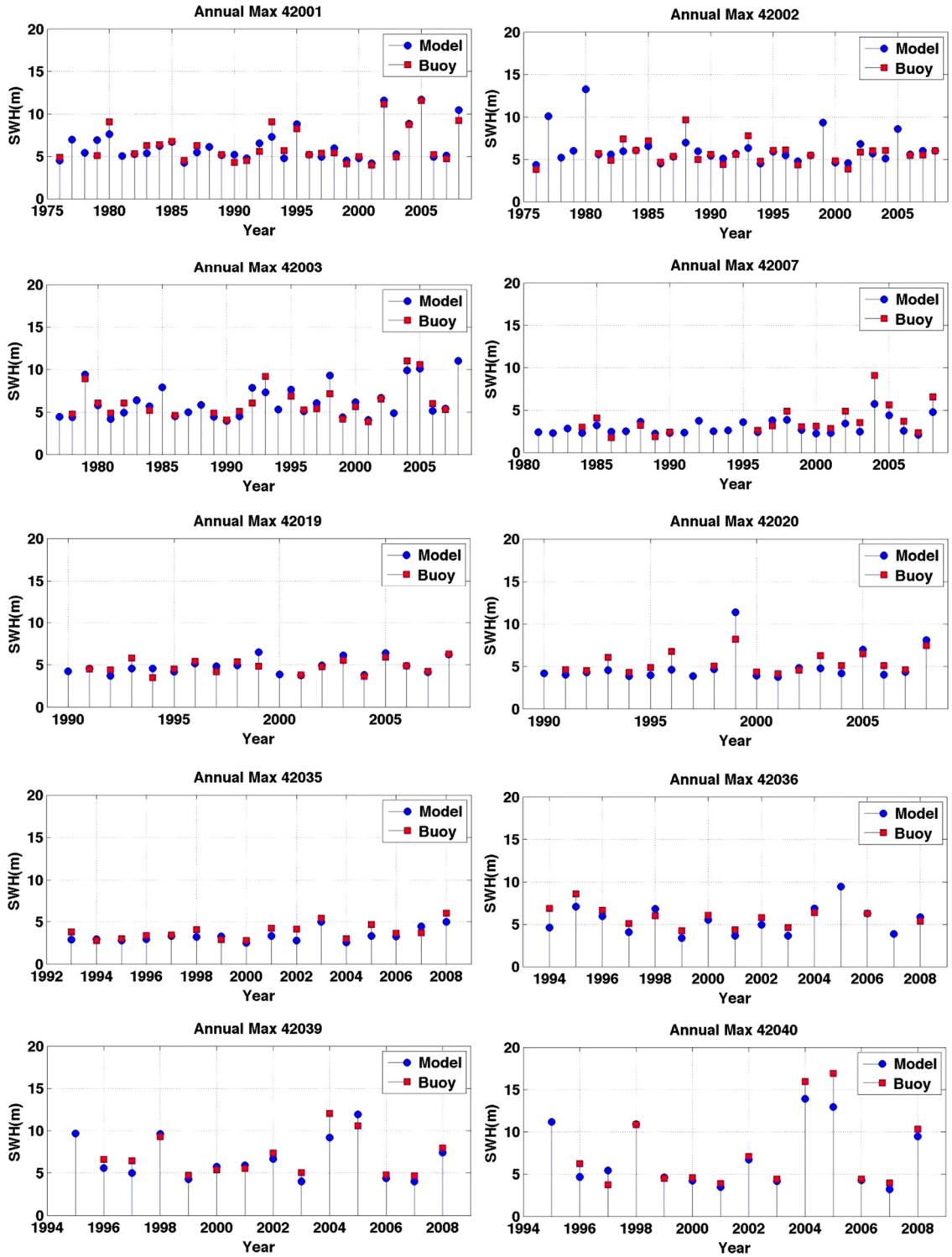

Fig. 13 Modeled and buoy annual maxima

Fortunately, as noted earlier, there are 11 NDBC wave buoys in the GOM (Fig. 2) and some of them have been recording data since 1976 (Table 1), creating a database that is sufficiently long for SWH_{100} estimation. In some cases the rule of thumb for extrapolating to duration three times the length of the data is satisfied. In fact, Palao et al. [2] and Panchang et al. [3] have used these data to obtain such estimates. Thus these data can be used to estimate SWH_{100} as a means to cross-check model-derived estimates. And, since the buoy data are available for varying lengths of time, the dependence of the errors on the length of the dataset can be assessed.

While buoy data may appear to have no problems such as modeling errors, other problems associated with them can influence a comparison of data-derived and model-derived SWH_{100} estimates. Typical problems found were as follows. First, there are frequent gaps in the data (Table 4). The gaps are sometimes for several months (which include the hurricane season) or for several hours (including in some cases the peak of a storm). Second, there can

Downloaded From: http://offshoremechanics.asmedigitalcollection.asme.org/ on 03/12/2014 Terms of Use: http://asme.org/terms

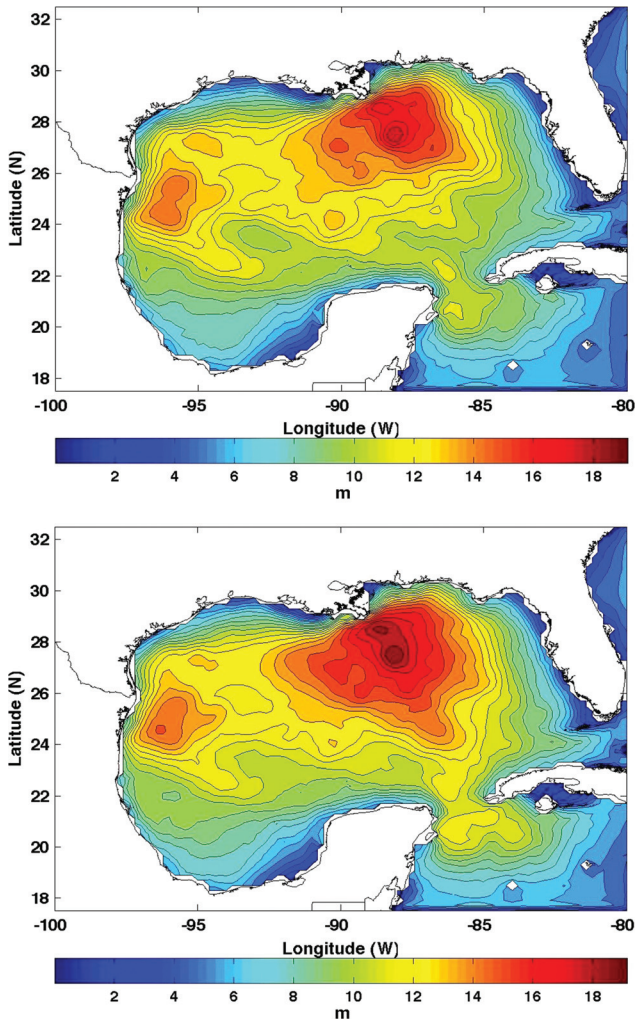

Fig. 14 Estimated SWH_{100} using the Gumbel method and 46 years (*a*) and 51 years (*b*) of data

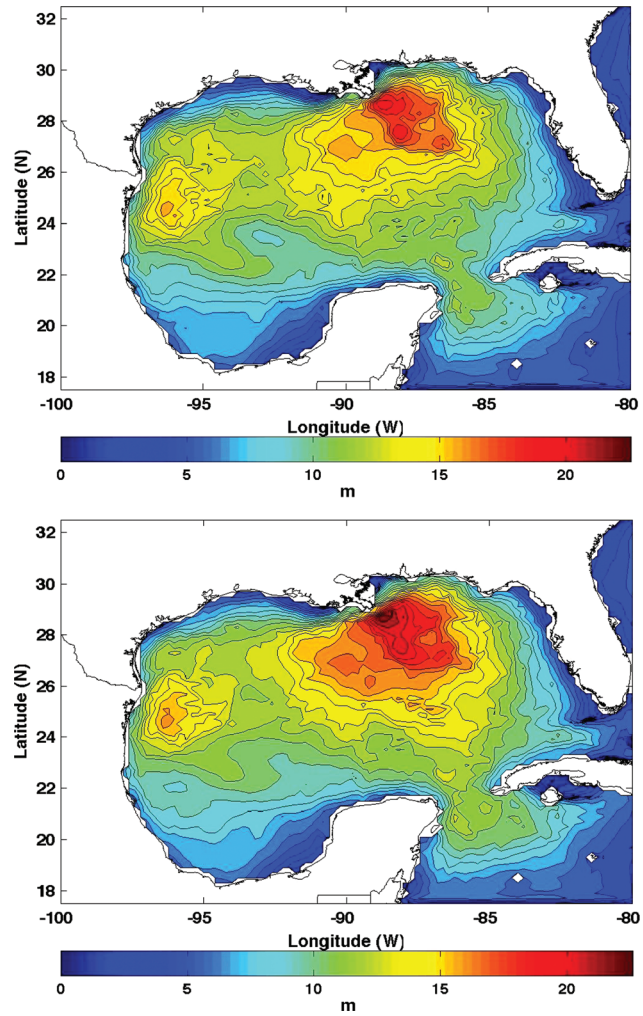

Fig. 15 Estimated SWH_{100} using the Weibull method and 46 years (*a*) and 51 years (*b*) of data

be uncertainties about the measurement location. This is sometimes due to a deliberate relocation of the buoy by NOAA, and at other times due to a considerable drift of the buoy in a storm. During Hurricane Ike (2008), for example, buoy 42,035 drifted approximately 40 km from its original location. If the buoy is located near the storm track, where the wave height variability is greater, the effect of such location changes on SWH_{100} comparisons at a prechosen point (we used a single location for each buoy) can be substantial. Finally, the quality of the measurements may have changed over the years and some measurements could be erroneous (Bender et al. [42]). Therefore, even though the buoys provide 'data', estimates obtained from these cannot be regarded as the 'absolute', but perhaps as a generally more 'reliable' value compared with models. A further point to be noted is that when making comparisons between model and buoy-derived SWH_{100} estimates is that the buoy location does not usually coincide with a model grid point. Here, the model grid point closest to the buoy was used, and the distance between the two varied between 3.6 km and 20 km. In addition, if the location happens to be near the storm track, the variability in the wavefields can create large differences in the two estimates.

Data from all eleven buoys were carefully examined and obvious problems were identified. When data during hurricane months was missing, model results for those months were used to assess the usability of a particular buoy. If model results (or HURDAT data) suggested that very large SWH's may have occurred during such periods, the remaining buoy data are not useful for estimation of SWH_{100}. A summary of the examination is provided in Table 4. On the basis of information contained therein, data from buoy 42,041 were discarded. For the other ten buoys, the annual maxima were used with the Gumbel, the Weibull, and the GEV distributions as described in Sec. 4. Estimates of SWH_{100} were obtained for the period excluding the years 2004–2008 and then by including them. Results were obtained using both buoy data and model data. For the model data, length of the dataset chosen corresponded to the earliest and latest buoy data availability.

Several features are apparent in the results which are presented in Table 5. First, at most locations, the SWH_{100} estimates obtained using buoy data and model data are close to each other for the most part, especially for the Gumbel and Weibull distributions. The differences are of the order of 10%. Frequently, the buoy-derived SWH_{100} is smaller than model SWH_{100}, which in some cases is probably a result of missing buoy data. This is likely in the case of buoys 42,001, 42,002, and 42,003 where at times annual maxima of the order of 7 m (based on model calculations) were missing. The differences between buoy and model SWH_{100} are certainly larger in the case of 42,020. The reasons for this were examined. Figure 13 shows a plot of the modeled and buoy annual maximum. It appears that one data point is responsible for this mismatch, i.e., year 1999, where the modeled SWH is 12 m as against the buoy SWH of 8 m. However, on examination this buoy was found to be close to the track of Hurricane Bret, and in a region of considerable wave height variability as seen in model

Downloaded From: http://offshoremechanics.asmedigitalcollection.asme.org/ on 03/12/2014 Terms of Use: http://asme.org/terms

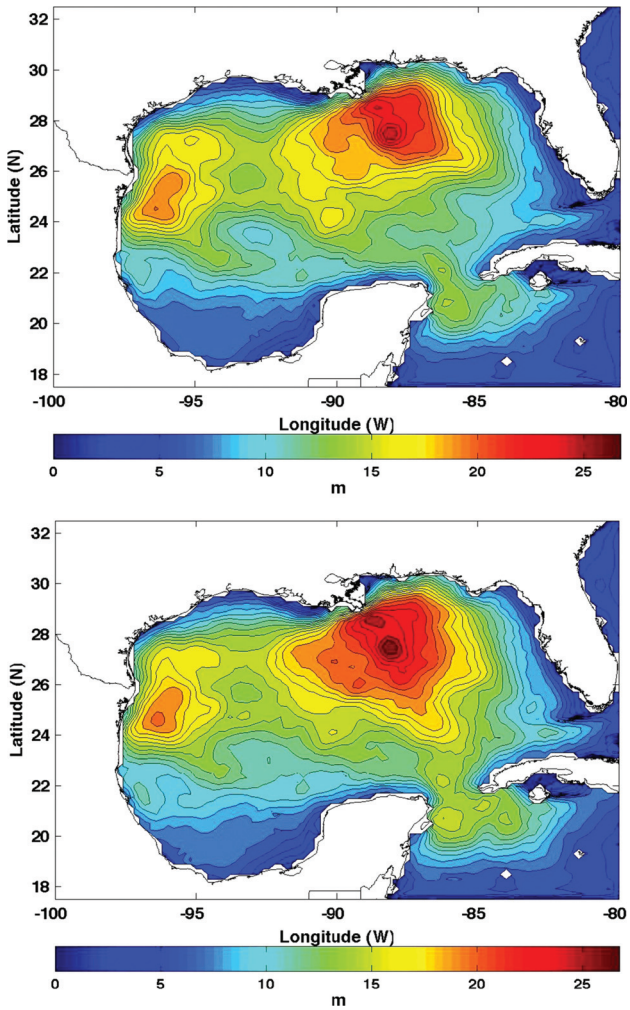

Fig. 16 Estimated SWH_{100} using the GEV method and 46 years (*a*) and 51years (*b*) of data

results. (Recall the issues pertaining to track uncertainty noted in Sec. 3; furthermore, the buoy location and the closest grid point are separated by about 12.8 km.) As an experiment, the effect of replacing the modeled value at this location with the buoy value was studied (denoted by model* in Table 5). The resulting model SWH_{100} were then much closer to buoy SWH_{100}, as shown in Table 5. This demonstrates the considerable effect of modeling errors when the dataset is a relatively short, as opposed to much smaller effect in the case of buoy 42,001, 42,002, and 42,003 where the longer dataset better corresponds to the rule of thumb. The difference for buoy 42,020 between the two models is smaller as the duration increases to include the 2004–2008 period (Table 5, right), indicating the diminishing importance of isolated large errors. The table also shows that the differences between buoy and model SWH_{100} are greater for the GEV distributions than for the other two distributions. The reason for this is that for the GOM, the GEV appears to emphasize the 'upper tail', as shown later in Sec. 6.

Finally, we see that the effect of the 2004–2008 periods is to increase the SWH_{100} at most locations, generally by about 2 m or less (based on the buoy data). At the location of buoy 42,040, however, the effect is much greater (e.g., using the Gumbel distribution the buoy SWH_{100} increases from ~13 m to ~22 m). This can be attributed to two reasons: very large wave heights were recorded in 2004–2008, and the data length is short. Adding the high SWH period of 2004–2008 increases the data length from only 8 years to 13 years. When the datasets are longer the effect of the 2004–2008 seasons is smaller.

Table 6 Estimated maximum SWH_{100} values

	1958–2003	1958–2008
Gumbel	18.2 m	19.1 m
Weibull	19.9 m	22.6 m
GEV	25.4 m	26.7 m

Overall, the similarity of the model-derivedand buoy-derived SWH_{100} values shown in Table 5 for the Gumbel and Weibull distributions for both periods is a validation of the modeling procedure. Further, we see that the effect of individual errors diminishes as the data length increases. In consequence, the three distributions are applied using all the model data developing Sec. 3 for 51 years.

7 Results and Discussion: SWH 100 Estimates for the GOM

After all the simulations were completed, a dataset for each grid point consisting of 51 annual maxima was developed. For each of the 7676 grid points, the 3 distributions described in Sec. 5 were fitted to the data and the SWH_{100} was estimated, and the bootstrap technique was used to identify the preferred distribution.

The SWH_{100} estimated by three different distributions are shown in Figs. 14–16 using both the pre-2004 data and the data that includes the 2004–2008 seasons. The maximum estimate (spatially) obtained with the Gumbel distribution is the smallest and that with GEV is the largest (Table 6). In these two cases, the effect of the 2004–2008 seasons is to increase maximum SWH_{100} estimate by 0.9 m and 1.3 m, respectively. The effect of the 2004–2008 season is more pronounced in the case of the Weibull distribution (maximum difference of 2.7 m) and the spatial variability of the differences is also greater, suggesting that the Weibull distribution has much greater sensitivity to the data than the other two.

The estimates of SWH_{100} provided in API [1,15] and Berek et al. [14] appear to suggest a maximum difference in the SWH_{100} of the order of 3.8 m. Calculations provided in Figs. 14–16 and Table 6 indicate that the effect of the 2004–2008 hurricane season is somewhat less. This would suggest that the differences in the SWH_{100} described in the two API publications may not be entirely due to the 2004–2008 hurricane season but could also be an effect of the approach taken to obtain the estimates, i.e., differences in the datasets as well as the distributions used may have contributed to the differences.

To summarize, Figs. 14–16 provides a range of SWH_{100}'s in the Gulf of Mexico. The range for the maximum SWH_{100} is as shown in Table 5. It is interesting to note from Figs. 14–16 that these maxima occur just south of Louisiana; no estimates for the area have been provided by API [15] (2007). However, estimates obtained by MacAfee and Wong [55] in this region are of the order of over 20 m, which are consistent with the results in Table 6.

While multiple estimates have been developed in Table 6, the question of which distribution is to be preferred remains. While there can be no absolute answer to this question, as explained in Sec. 4, the bootstrap technique provides some guidance. 500 samples were generated using the data at each grid point and the error norm calculated for six values of h (0.35, 0.5, 0.75, 1, 1.25, and 1.5); the distribution with the least error norm is selected. The results, shown in Fig. 17, indicate that for small values of h the Gumbel distribution is the preferred one, and for $h > 1$, the GEV is the preferred distribution. As h increases from small values, at many locations, the Weibull and the GEV are the preferred distributions (Fig. 17).

Recalling that small values of h correspond to an emphasis on the lower tail and $h > 1$ corresponds to an emphasis on the upper

Downloaded From: http://offshoremechanics.asmedigitalcollection.asme.org/ on 03/12/2014 Terms of Use: http://asme.org/terms

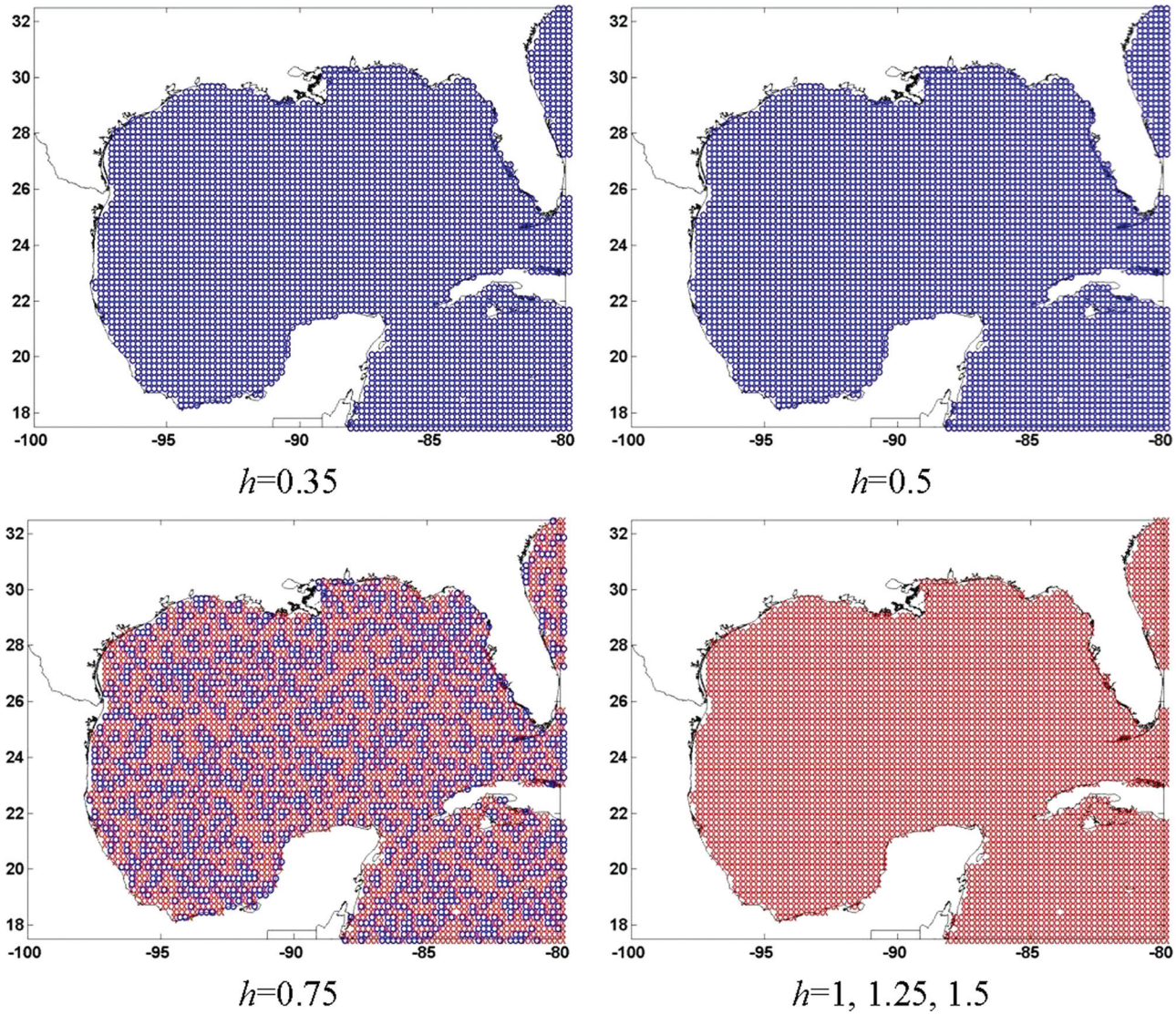

Fig. 17 Variation of optimal distribution with *h* (GEV: red, Gumbel: blue)

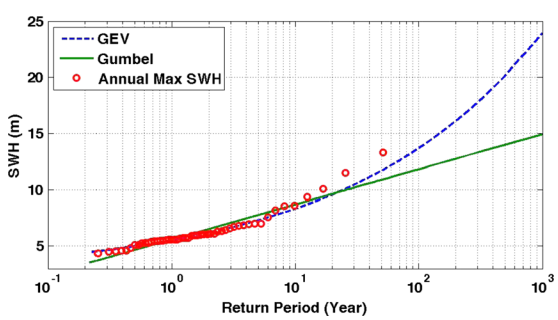

Fig. 18 SWHs corresponding to different return periods

tail, the smooth progression between the distributions observed in Fig. 17 implies that the Gumbel and the GEV are the two extremes. This allows the engineer to make a reasoned selection, i.e., if one wants to emphasize the lower tail (where most of the data lie), then the Gumbel distribution is to be preferred, as illustrated by Fig. 18. However, if a better fit to the larger data values is to be emphasized, the GEV would be the preferred choice (Fig. 18).

Table 7 shows a comparison between the three different methods and API [15] estimates. (The latter are estimated from the plots in API [15] near the locations of the eleven buoys.) The GEV estimates are, for the most part, higher than the API estimates. Note that in shallow areas (e.g., near buoys 42,007 and 42,035, where the depth is ~ 14 m), the addition of a 5 m storm surge could result in a 1 m increase in the SWH_{100}. It is interesting that the Weibull results obtained here (for 51 years) are mostly close to (but somewhat larger than) the API results [15]. (With the exception buoy 42,041, the difference is less than about 2 m.) The API study also used the Weibull distribution and though their dataset and modeling methods are different and their statistical analysis could be sensitive to the threshold chosen, it is encouraging that the two sets reinforce each other. While our maximum Weibull estimate (22.6 m) is considerably greater than the maximum (15.8 m) reported by Berek et al. [14], it must be noted that the API [15] does not provide results for certain areas where our calculations show large SWH_{100} values (south of Louisiana). Also, as noted above, the Weibull results appear to be the most sensitive to the data (suggesting perhaps that the other distributions may be more robust), and the GEV, which provides a better fit to the larger data values (e.g., Fig. 18), may provide a reasonable and conservative alternative to the engineer. In the case of the GEV, though, it must be noted that a better fit to the higher data values implies larger estimates if N (the return period) is much greater than the data length. Because of the nonlinear

Downloaded From: http://offshoremechanics.asmedigitalcollection.asme.org/ on 03/12/2014 Terms of Use: http://asme.org/terms

Table 7 Comparison of estimated SWH_{100} (m) at NDBC buoy locations

	GEV		Gumbel		Weibull		API		
Buoy no.	46 year	51 year	46 year	51 year	46 year	51 year	RP2-WSD	2INT-MET	MAX SWH
42001	16.53	17.10	13.35	13.83	14.30	14.97	11.9	15.2	11.63
42002	13.82	13.65	11.88	11.78	11.81	11.69	11.9	12.3	9.7
42003	15.78	16.58	12.42	13.17	13	14.08	11.9	13.03	11.04
42007	7.79	7.87	6.51	6.81	7.07	7.62	NA	NA	9.09
42019	13.37	12.89	10.84	10.65	11.31	11.19	10.5	11.6	6.3
42020	15.48	15.92	11.8	12	11.81	12.19	10.6	11.8	8.2
42035	6.68	6.88	5.75	5.97	5.78	6.08	5.3	7.44	7.1
42036	12.63	12.8	10.5	10.85	11.81	12.34	11.8	10.2	8.6
42039	16.43	18.84	12.75	14.34	14.05	15.79	11.8	13.77	12.05
42040	19.09	20.37	14.28	15.44	16.24	18.33	11.9	NA	16.91
42041	18.78	19.61	14.58	15.26	15.32	16.22	11.9	12.44	12.31

nature of the curve in Fig. 18, it is not reasonable to obtain estimates for return periods of the order of 200, 500 and even 1000 years as provided in API [15].

8 Summary and Conclusions

In this study, SWH estimates at 7676 grid points in the GOM were obtained using a combination of the modified Rankine Vortex model (Jeong et al. [23]) and the reanalysis dataset, along with the SWAN wave model, for the 1958–2008 periods. The modeled wind and wave height data were validated using nearly all the data available. Analyses of these data lead to the following conclusions:

(1) Modeled monthly maximum SWH values, when compared with corresponding buoy data (available up to 33 years), yielded a slope of 0.82 (based on 2760 points), indicating a high correlation. The mismatch was due partly to storm track uncertainty, separation between the chosen grid point and the buoy, and the large wave height variability near the storm track.

(2) Model results for 51 years at 7676 grid points show that the maximum modeled SWH is 18 m. The effect of the 2004–2008 seasons is not large on the maximum SWH in the GOM, but the frequency of large waves (SWH > 10 m) increased substantially. Also, the eastern part of the GOM shows an increasing trend while the western part a decreasing trend. In the eastern part, the maximum trend is approximately 5.6 cm/year in the maximum SWH (based on 51 years), 1.77 cm/year based on the 1975–2004 period, and 4.84 cm/year based on the 1975–2008 period. The numbers that include the latest time periods are comparable to estimates obtained for the west coast of the U.S. (e.g., Graham [9]; Ruggiero et al. [11]). The trends can be used for obtaining time-dependent estimates of extreme wave estimates; this type of estimation is receiving greater prominence owing to sea level rise and climatic changes (e.g., Obeysekera et al. [13]; Warner and Tissot [12]).

(3) SWH_{100} were obtained using annual maximum obtained by modeling and from buoy data. The buoy data lengths varied from 10 years to 33 years. The SWH_{100} estimates mostly increased upon inclusion of the 2004–08 hurricane season. The SWH_{100} estimates obtained using the two datasets are mostly consistent, with a maximum difference of 2 m (for the most part). This consistency is a validation of the model-derived data for statistical analysis. Using buoy 42,020 as an example, it was seen that errors in individual modeled SWHs have a decreasing effect on SWH_{100} as the data length increased from 1990–2003 to 1990–2008.

(4) The revised API manual [15] notes that statistical methods other than those used in their study can yield slightly different results. This study explored a range of alternative estimates. In addition, efforts were directed toward identifying the preferred distribution. SWH_{100} estimates were obtained using 46 and 51 years of model data. The Weibull estimates were similar to (but somewhat larger than) the revised API estimates (also obtained with the Weibull distribution but using different data and statistical methods). The bootstrap method indicated that, for all grid points, the GEV distribution is to be preferred if the emphasis is on the larger wave heights where extreme occur, and the Gumbel distribution is to be preferred if the emphasis is on the lower tail. The maximum increase caused by the 2004–2008 season in the SWH_{100} is approximately 2.7 m (for the Weibull distribution), 1.3 m (for the GEV distribution), and 0.9 m (for the Gumbel distribution). These are smaller than the difference between the old and new API guidelines. The 2004–2008 seasons resulted in greater spatial variability of the SWH_{100} estimates. Table 5 and Figs. 16–18 provided alternative estimates for SWH_{100} in the GOM. The maximum SWH_{100} estimates using the three methods are 19.1 m, 22.6 m, and 26.7 m (Gumbel, Weibull, and GEV); while these estimates are larger than the revised API estimates, it is noted that the latter are not available for all areas of the GOM.

Acknowledgment

This work is an outgrowth of coastal wave prediction work supported by the Texas Coastal Management Program (NOAA). Zeki Demirbilek is grateful for the technical support received in this activity from two research programs of the U.S. Army Corps of Engineers: Coastal Inlets Research Program (CIRP), and Dredging Operations and Environmental Research (DOER). Permission to publish this paper was granted by the Chief, Army Corps of Engineers.

References

[1] American Petroleum Institute (API), 2000, "Recommended Practice for Planning, Designing and Constructing Fixed Offshore Platforms—Working Stress Design," API Recommended Practice 2A-WSD, Washington, DC.

[2] Palao, I. M., Teng, C. C., and Brown, D. A., 1994, "An Extremal Analysis of Significant Wave Height Data Measured From NDBC Buoys," Report No. 1804-07.01, NDBC, Stennis Space Center, MS, p. 46.

[3] Panchang, V. G. L., Zhao, L., and Demirbilek, Z., 1999, "Estimation of Extreme Wave Heights Using GEOSAT Measurements," Ocean Eng., **26**, pp. 205–225.

[4] Wang, D. W., Mitchell, D. A., Teague, W. J., Jarosz, E., and Hulbert, M. S., 2005, "Extreme Waves Under Hurricane Ivan," Science, **309**, p. 896.

[5] Hovis, G. T., 2005, "Analysis of Storm Surge Measured at Water Level Stations From Hurricanes Charley, Frances, Ivan, and Jeanne," Proc. Solutions to Coastal Disasters 2005, ASCE, Reston, VA, p. 1–15.

[6] Panchang, V. G., and Li, D., 2006, "Large Waves in the Gulf of Mexico Caused by Hurricane Ivan," Bull. Am. Met. Soc., **87**(4), p. 481–489.

Downloaded From: http://offshoremechanics.asmedigitalcollection.asme.org/ on 03/12/2014 Terms of Use: http://asme.org/terms

[7] Clayton, B., 2007, "Gearing up for Gulf Hurricanes," *Houston Chronicle*, Apr 29.
[8] Wang, X. L., Zwiers, F. W., and Swail, V. R., 2004, "North Atlantic Ocean Wave Climate Change Scenarios for the Twenty-First Century," J. Climate, **17**(12), pp. 2368–2383.
[9] Graham, N., 2005, "Coastal Impacts of North Pacific Winter Wave Climate Variability: The Southern California Bight and the Gulf of Farallones," Report No.CEC-500-2005-018, Scripps Institution of Oceanography and Hydrologic Research Center, State of California Energy Commission, San Diego, CA, p. 34.
[10] Komar, P. D., and Allan, J. C., 2007, "Higher Waves Along US East Coast Linked to Hurricanes," EOS Trans., **88**(30), p. 301.
[11] Ruggiero, P., Komar, P. D., and Allan, J. C., 2010, "Increasing Wave Heights and Extreme Value Projections: The Wave Climate of the U.S. Pacific Northwest," Coastal Eng., **57**, pp. 539–552.
[12] Warner, N. N., and Tissot, P. E., 2012, "Storm Flooding Sensitivity to Sea Level Rise for Galveston Bay, Texas," Ocean Eng., **44**, pp. 23–32.
[13] Obeysekera, J., Park, J., Irizzary-Ortiz, M., Barnes, J., and Trimble, P., 2013, "Probabilistic Projection of Mean Sea Level and Coastal Extremes," J. Waterways, Port, Coastal Ocean Eng., **139**, pp. 135–141.
[14] Berek, E. P., Cooper, C. K., Driver, D. B., Heideman, J. C., Mitchell, D. A., Stear, J. D., and Vogel, M. J., 2007, "Development of Revised Gulf of Mexico Metocean Hurricane Conditions for Reference by API Recommended Practices," Offshore Technology Conference (OTC), Houston, TX.
[15] American Petroleum Institute (API), 2007, "Interim Guidance on Hurricane Conditions in the Gulf of Mexico," API Bulletin 2INT-MET, Washington, DC.
[16] Pontes, M. T., Aguiar, R., and Oliveira Pires, H., 2005, "A Nearshore Wave Energy Atlas for Portugal," ASME J. Offshore Mech. Arct. Eng., **127**(3), pp. 249–255.
[17] Millar, D. L., Smith, H. C. M., and Reeve, D. E., 2006, "Modeling Analysis of the Sensitivity of Shoreline Change to a Wave Farm," Ocean Eng., **34**(5–6), pp. 884–901.
[18] Panchang, V. G., Jeong, C., and Li, D., 2008, "Wave Climatology in Coastal Maine for Aquaculture and Other Applications," Estuaries Coasts, **31**(2), pp. 289–299.
[19] Cieślikiewicz, W., and Paplińska-Swerpel, B., 2008, "A 44-Year Hindcast of Wind Wave Fields Over the Baltic Sea," Coastal Eng., **55**, pp. 894–905.
[20] Rogers, W. E., Kaihatu, J. M., Hsu, L., Jensen, R. E., Dykes, J. D., and Holland, K. T., 2007, "Forecasting and Hindcasting Wave With the SWAN Model in the Southern California Bight," Coastal Eng., **54**, pp. 1–15.
[21] Cardone, V. J., Greenwood, C. V., and Greenwood, J. A., 1992, "Unified Program for the Specification of Hurricane Boundary Layer Winds Over Surfaces of Specified Roughness," Army Engineer Waterways Experiment Station, Contract Report No. CERC-92-1, Vicksburg, MS.
[22] Forristall, G. Z., 2007, "Comparing Hindcasts With Wave Measurements From Hurricanes Lili, Ivan, Katrina and Rita," Proc. 10th International Workshop on Wave Hindcasting and Forecasting and Coastal Hazards Symposium, North Shore, Oahu, HI, Nov. 11–16.
[23] Jeong, C. K., Panchang, V. G., and Demirbilek, Z., 2012, "Parametric Adjustments to the Rankine Vortex Wind Model for Gulf of Mexico Hurricanes," ASME J. Offshore Mech. Arctic Eng., **134**(4), p. 041102.
[24] Powell, M. D., Houston, S. H., Amat, L. R., Morisseau-Leroy, N., 1998, "The HRD Real-Time Hurricane Wind Analysis System," J. Wind Eng. Indust. Aerodyn, **77–78**, pp. 53–64.
[25] Xu, S., and Huang, W., 2011, "Estimating Extreme Water Levels With Long-Term Data by GEV Distribution at Wusong Station Near Shanghai City in Yangtze Estuary," Ocean Eng., **38**(2–3), pp. 468–478.
[26] Van Vledder, G., Goda, Y., Hawkes, P., Mansard, E., Martin, M. J., Mathiesen, M., Peltier, E., and Thompson, E., 1993, "Case Studies of Extreme Wave Analysis: A Comparative Analysis," Proc. 2nd International Sympos. Ocean Wave Measurement and Analysis, ASCE, New York, pp. 978–992.
[27] Li, Y., Simmonds, D., Reeve, D., 2008, "Quantifying Uncertainty in Extreme Values of Design Parameters With Resampling Techniques," Ocean Eng., **35**, pp. 1029–1038.
[28] Borgman, L. E., 1975, "Extremal Statistics in Ocean Engineering," Civil Engineering in the Oceans Conference, New York, pp. 117–133.
[29] Kalnaya, M. K. E., Kistler, R., Collins, W., Deaven, D., Gandin, L., Iredell, M., Saha, S., White, G., Woollen, J., Zhu, Y., Leetmaa, A., Reynolds, R., Chelliah, M., Ebisuzaki, W., Higgins, W., Janowiak, J., Mo, K. C., Ropelewski, C., Wang, J., Jenne, R., Joseph, D., 1995, "The NCEP/NCAR 40-Year Reanalysis Project," Bull. Am. Met. Soc., **77**, pp. 437–471.
[30] Music, S., and Nickovic, S., 2008, "44-year Wave Hindcast for the Eastern Mediterranean," Coastal Eng., **55**, pp. 872–880.
[31] MacAfee, A. W., and Pearson, G. M., 2006, "Development and Testing of Tropical Cyclone Parametric Wind Models Tailored for Midlatitude Application—Preliminary Results," J. Appl. Meteor. Climatol., **45**, pp. 1244–1260.
[32] Xie, L., Bao, S., Pietrafesa, L. J., Foley, K., and Fuentes, M., 2006, "A Real-Time Hurricane Surface Wind Forecasting Model: Formulation and Verification," Mon. Weather Rev., **134**, pp. 1355–1370.
[33] Booij, N., Ris, R. C., and Holthuijsen, L. H., 1999, "A Third-Generation Wave Model for Coastal Regions: 1. Model Description and Validation," J. Geophys Res., **104**(C4), pp. 7649–7666.
[34] Ris, R. C., Holthuijsen, L. H., and Booij, N., "A Third-Generation Wave Model for Coastal Regions: 2. Verification," J. Geophys Res, **104**, pp. 7667–7681.
[35] Booij, N., Holthuijsen, L. H., Doorn, N., and Kieftenburg, A. T. M. M., 1997, "Diffraction in a Spectral Wave Model," *Ocean Wave Measurements and Analysis*, Proc. 3rd Internat'l Sympos. (Waves97), Virginia, ASCE, New York, pp. 243–255.
[36] Zubier, K., Panchang, V. G., and Demirbilek, Z., 2003, "Simulation of Waves at Duck (North Carolina) Using Two Numerical Models," Coastal Eng. J, **45**(3), pp. 439–469.
[37] Chen, Q., Zhao, H. H., Hu, K. L., and Douglass, S. L., 2005, "Prediction of Wind Waves in a Shallow Estuary," J. Waterway, Port, Coastal., Ocean Eng., **1341**(4), pp. 137–148.
[38] Singhal, G., Panchang, V. G., and Lillibridge, J., 2010, "Reliability Assessment for a Wave Forecasting System for Prince William Sound, Alaska," J. Waterway, Port, Coastal. Ocean Eng., **136**(6), pp. 337–349.
[39] Liu, H., Xie, L., Pietrafesa, L. J., and Bao, S., 2007, "Sensitivity of Wind Waves to Hurricane Wind Characteristics," Ocean Modelling, **18**, pp. 37–52.
[40] Heideman, J. C., and Mitchell, D. A., 2009, "Grid Point Pooling in Extreme Value Analysis of Hurricane Hindcast Data," J. Waterway, Port, Coastal, Ocean Eng., **135**, pp. 31–37.
[41] Jonathan, P., and Ewans, K., 2011, "A Spatiodirectional Model for Extreme Waves in the Gulf of Mexico," ASME J. Offshore Mech. Arct. Eng., **133**(1), p. 011601.
[42] Bender, L. C., Guinasso, N. L., Walpert, J. N., and Howden, S. D., 2010, "A Comparison of Methods for Determining Significant Wave Heights—Applied to a 3-m Discus Buoy During Hurricane Katrina," J. Atmos. Ocean. Technol., **27**(6), pp. 1012–1028.
[43] Earle, M. D., 1975, "Extreme Wave Conditions During Hurricane Camille," J. Geophys. Res., **80**(3), pp. 377–379.
[44] Kennedy, A. B., Gravois, U., and Zachry, B., 2011, "Observations of Landfalling Wave Spectra During Hurricane Ike," J. Waterway, Port, Coastal, Ocean Eng., **137**(3), pp. 142–145.
[45] Jeong, C. K., and Panchang, V. G., 2008, "Measurement-Based Estimates of Extreme Wave Conditions for the Gulf of Mexico," Oceans 2008 Conference, Quebec, MTS/IEEE.
[46] Neelamani, S., Al-Salem, K., and Rakha, K., 2007, "Extreme Waves for Kuwaiti Territorial Waters," Ocean Eng., **34**, pp. 1496–1504.
[47] Perez, O. M., Telfer, T. C., and Ross, L. G., 2003, "On the Calculation of Wave Climate for Offshore Cage Culture Site Selection: A Case Study in Tenerife," Aquacultural Eng., **29**, pp. 1–21.
[48] Federal Emergency Management Agency, 2004, "Final Draft Guidelines for Coastal Flood Hazard Analysis and Mapping for the Pacific Coast of the United States," FEMA Study Contractor: Northwest Hydraulic Consultants, Inc.
[49] Carter, D. J. T., and Challenor, P. G., "Estimating Return Values of Environmental Parameters," Q. J. R. Meteorol. Soc., **107**, pp. 259–266.
[50] Jonathan, P., Ewans, K., and Forristall, G., 2008, "Statistical Estimation of Extreme Ocean Environments: The Requirement for Modelling Directionality and Other Covariate Effects," Ocean Eng., **35**(11–12), pp. 1211–1225.
[51] Jonathan, P., and Ewans, K., 2011, "Modeling the Seasonality of Extreme Waves in the Gulf of Mexico," ASME J. Offshore Mech. Arct. Eng., **133**(2), p. 021104.
[52] Mackay, E. B. L., Challenor, P. G., and Bahaj, A. S., 2010, "On the Use of Discrete Seasonal and Directional Models for the Estimation of Extreme Wave Conditions," Ocean Eng., **37**(5–6), pp. 425–442.
[53] Jonathan, P., and Ewans, K., 2011, "Discussion of 'On the Use of Discrete Seasonal and Directional Models for the Estimation of Extreme Wave Conditions' by Edward B. L. Mackay, Peter G. Challenor, AbuBakr S. Bahaj [Ocean Eng., **37**(5–6), 2010, pp. 425–442]," Ocean Eng., **38**(1), 1, p. 205.
[54] Petrauskas, C., and Aagaard, P. M., 1971, "Extrapolation of Historical Storm Data for Estimating Design-Wave Heights," Soc. Pet. Eng. J., **11**, pp. 23–37.
[55] MacAfee, A. W., and Wong, S. W. K., 2007, "Extreme Value Analysis of Tropical Cyclone Trapped-Fetch Waves," J. Appl. Meteor. Climatol., **46**, pp. 1501–1522.

Downloaded From: http://offshoremechanics.asmedigitalcollection.asme.org/ on 03/12/2014 Terms of Use: http://asme.org/terms